Solvation Dynamics in Mixtures of Polar and Nonpolar Solvents

F. Cichos, A. Willert, U. Rempel,* and C. von Borczyskowski

Institut für Physik 13303, Technische Universität Chemnitz-Zwickau, D-09107 Chemnitz, Germany

Received: May 20, 1997[⊗]

Time-resolved Stokes shift measurements and steady-state absorption and fluorescence measurements of Coumarin 153 (C153) at different temperatures were used to explore the solvation dynamics of binary mixtures of alcohols and alkanes at various alcohol concentrations. These solvent mixtures show even at alcohol concentrations as low as 0.3% a strong Stokes shift of about 1200 cm^{-1}. Depending on alcohol concentration, this Stokes shift takes place on a time scale ranging from 300 ps up to several nanoseconds. These characteristic times are 2 orders of magnitude longer than the relaxation times typically found in alcohols, which is attributed to rotational reorientation of the solvent molecules. A monoexponential temporal behavior of the Stokes shift and a linear dependence of the time constants on the alkane viscosity are observed. These results and temperature dependent static fluorescence measurements strongly support a diffusion-controlled process of solvation in these mixtures.

1. Introduction

The importance of solvents in chemistry is widely discussed in the literature.[1] Solvents alter the pathways of reactions, change the energies of the reactants, and contribute to the stability of the final states of a reaction (e.g. in electron-transfer reactions). This importance is one of the reasons for the research in the field of solvation and solvation dynamics. Solvation has been explored for a long time via the shift of the static absorption and fluorescence spectra of probe molecules relative to the gas-phase spectra in different solvent environments.[2−6] The development of pulsed laser systems focused the interest on measurements of solvent dynamics.[7,8] Only recently, ultrashort laser pulses made it possible to study solvation processes on a sub-picosecond time scale predicted from theoretical studies.[9,10] In many investigations of solvation dynamics the time dependent Stokes shift of the fluorescence band of a probe molecule dissolved in the solvent under study is measured.[11,12] This probe solute (usually a laser dye) is excited by a short laser pulse. Due to a redistribution of the electron density, the dipole moment of the solute changes during the excitation. The solvent environment cannot follow the sudden change in the dipole moment, and so a nonequilibrium state is created. During the relaxation of the solvent toward a new equilibrium state the interaction energy between solvent and solute changes and the fluorescence band of the dye shifts.

Until now there have been a lot of investigations of solvent dynamics measurements in pure polar solvents,[9,13−16] while there are only a few studies of solvation dynamics in nonpolar solvents[17−19] or in mixtures of nonpolar and polar solvents.[20] The diffusive solvent relaxation (on the time scale of a few picoseconds or longer) in pure polar liquids is usually considered as a reorientation of the solvent molecules surrounding the dye probe molecule. A mixture of a polar and a nonpolar solvent requires the consideration of translational diffusion processes, too, as these control the dynamics of dielectric enrichment in the solvation shell. Up to now this solvation controlled by translational diffusion was only rarely studied.[20] Separating both processes, reorientation of the solvent shell molecules and translational diffusion controlled solvation, may on one hand allow the investigation of the behavior of a single solvation shell and on the other hand give information about the structure of polar molecules in nonpolar surroundings.

In simple continuum theory, where a dipolar interaction is considered the only important interaction, the effect of the solvent on the probe molecule energy is given by

$$E = \frac{-\mu^2 f(\epsilon)}{8\pi\epsilon_0 a^3} \tag{1}$$

where μ is the probe molecule's static dipole moment, a^3 is its volume, and $f(\epsilon)$ is the Onsager function of the dielectric constant of the solvent ϵ.

$$f(\epsilon) = \frac{2(\epsilon - 1)}{2\epsilon + 1} \tag{2}$$

In the case of a homogeneous mixture of a nonpolar (N) and a polar (P) solvent around the solute the effective Onsager function should be a simple linear combination of the Onsager functions of both solvent parts according to the mole fractions x_P, x_N of the two solvent components.

$$f(\epsilon_m) = x_N f(\epsilon_N) + x_P f(\epsilon_P) \tag{3}$$

From dielectric measurements it is known that eq 3 applies to some mixtures (which are therefore said to behave ideally), while for certain cases deviations from eq 3 are observed, indicating an inhomogeneous (structured) mixture of the two solvents.[21] When the probe solute for Stokes shift measurements does not disturb the solvent structure, the solvatochromic shift of a fluorescence or absorption band is linear with respect to the polar solvent mole fraction x_P. On the other hand a local enrichment of one solvent component around the solute, which is called "preferential solvation", will lead to deviations from this linear dependence.[21] This happens due to various interactions (i.e. electrostatic forces, hydrogen bonding) of the solute with the two different solvent components. In most cases strong dipole moments of the polar solvent component and the solute cause this enrichment. The result is that the solute interacts with a higher mole fraction of this component than exists in the "bulk" of the solvent mixture. Due to this preferential solvation, the solvatochromic shift is not proportional to the

* To whom correspondence should be addressed.

[⊗] Abstract published in *Advance ACS Abstracts,* October 1, 1997.

S1089-5639(97)01669-1 CCC: $14.00

bulk mole fraction x_P. The deviation from the linear behavior is a measure of the strength of the preferential solvation.

It is the aim of our measurements to understand the solvent relaxation in binary mixtures of alkanes and alcohols. Section 2 describes the experimental setup and the data analysis. In section 3 we present the data obtained from steady-state fluorescence and absorption measurements as well as results from time-resolved Stokes shift measurements. A detailed discussion of the data in comparison to the above-described models of binary mixtures follows in section 4.

2. Experimental Methods and Data Analysis

(a) Setup. The experimental setup for the time-resolved measurements consists of a mode-locked titanium−sapphire laser (Coherent Mira Model 900B) pumped by a multiline Ar^+ laser (Coherent Innova 310, $P_{cw} = 8$ W). The titanium−sapphire laser delivers pulses with a duration of about 120 fs and a repetition rate of 76 MHz. The output power at 800 nm wavelength is 1 W(13 nJ/pulse). The repetition rate is reduced by a factor of 5 with an electrooptic modulator (Conoptics 305). To excite the dye, the second harmonic of the Ti:Sa beam is generated in a 2 mm LBO crystal. The pulses are focused into the sample in a 10 × 10 mm cuvette. Before reaching the detection system, the fluorescence light passes a polarization filter at the magic angle. The detection system consists of a monochromator (Chromex 250IS) and a streak scope (Hamamatsu C4334). The streak scope directly delivers a two-dimensional image of the time and wavelength dependence of the fluorescence light. This image is resolved in an CCD array of 480 × 640 pixels, along the time and wavelength axes, respectivly. The wavelength range used in this study is from 372 to 653 nm. The maximum time resolution (system response time) which can be obtained is approximately 30 ps.

The static spectra were recorded on a spectrofluorometer (Shimadzu RF-5001PC) and an absorption spectrophotometer (Shimadzu UV-3101PC). Temperature dependent measurements were done with homemade cryostats. Coumarin 153 was obtained from Lambda Physics and used without further purification. Solvents were obtained from Merck or Aldrich (spectroscopic grade) and used as delivered.

(b) Data Analysis. Usually the shape of the C153 fluorescence band is well described by a log-normal function.[11]

$$f(\nu) = \begin{cases} g_0 \exp\left\{-\ln(2)\left(\dfrac{\ln[1+2b(\nu-\nu_0)/\Delta]}{b}\right)^2\right\} & \text{if } 2b(\nu-\nu_0)/\Delta > -1 \\ 0 & \text{otherwise} \end{cases} \quad (4)$$

Here Δ represents the bandwidth, b the asymmetry, and ν_0 the position of the maximum of the band. Fitting $f(\nu)$ to the data at each time step yields the parameters ν_0, Δ, and b as a function of time.

Our experiments showed that the fluorescence of C153 in hexane/alcohol mixtures has a clearly visible vibronic structure which disappears with increasing alcohol concentration or delay after excitation. The nonstructured fluorescence data, but not the structured spectra, were well represented by the log-normal curve. To obtain comparable values for the center, width, asymmetry, and intensity for structured and nonstructured spectra, we replaced the fitting with a log-normal function by a momentum analysis method as described in ref 22. This method calculates the mean value m (eq 6) and the two central moments μ_2, μ_3 (eqs 7, 8) weighted by the fluorescence intensity. The second central moment, μ_2, is the standard deviation from the mean (width of the fluorescence band). The third moment, μ_3, describes the asymmetry of the fluorescence band.

$$I_t = \sum_i I(\tilde{\nu}_i)\Delta\tilde{\nu}_i \quad (5)$$

$$m = \sum_i \tilde{\nu}_i I(\tilde{\nu}_i)\Delta\tilde{\nu}_i \quad (6)$$

$$\mu_2 = \left(\frac{\sum_i (\tilde{\nu}_i - m)^2 I(\tilde{\nu}_i)\Delta\tilde{\nu}_i}{I_t}\right)^{1/2} \quad (7)$$

$$\mu_3 = \left(\frac{\sum_i (\tilde{\nu}_i - m)^3 I(\tilde{\nu}_i)\Delta\tilde{\nu}_i}{I_t}\right)^{1/3} \quad (8)$$

Additionally, the sum (eq 5) of the fluorescence intensity at all wavenumbers gives information about the fluorescence lifetime of the dye. To analyze the results at each of the 480 time channels, a spectrum $I(\lambda)$ is taken from the streak scope image and converted to a wavenumber scale by $I(\tilde{\nu}) = \lambda^2 I(\lambda)$. The described spectral parameters were calculated for each spectrum $I(\tilde{\nu})$ and the time constant for the Stokes shift τ_S was determined by fitting the time dependent mean value m to a monoexponential function.

3. Results

3.1. Steady-State Spectra. 3.1.1. Absorption and Fluorescence Spectra at Room Temperature. Steady-state absorption spectra of C153 were measured in mixtures of hexane/methanol, hexane/ethanol, and hexane/heptanol at different alcohol concentrations. Due to the low solubility of methanol (MeOH) in hexane, the concentration range was limited in this case to mole fractions from 0 to 0.12, while for the other alcohols the complete range of $x_P = 0, ..., 1$ could be covered. In all solvent mixtures C153 spectra show the same general dependence on the alcohol concentration. In pure hexane the absorption spectrum is centered at 25 960 cm^{-1} (first moment) and shows a clearly resolved vibrational structure with maxima at 24 330 and 25 560 cm^{-1}. At low alcohol concentrations ($x_P < 0.1$) this vibronic structure is still visible. Only a slight shift is observed in this concentration range, but the intensity of the long wavelength band increases compared to the short wavelength band. At higher alcohol concentrations the vibrational structure vanishes and the whole spectrum undergoes a pronounced red-shift. The maximum shift between the spectra of C153 in pure hexane and in the pure alcohol varies with the alcohol polarity, as is well-known.[9] Figure 1a shows as a representative example the normalized absorption spectra in a hexane/heptanol mixture at different heptanol (HepOH) mole fractions.

Steady-state fluorescence spectra were recorded for the same mixtures as the steady-state absorption spectra. The vibrational structure, which is observed in pure hexane (center 21 870 cm^{-1}, vibrational bands at 22 240 and 23 100 cm^{-1}), vanishes faster with increasing alcohol concentration than in the absorption spectra. Accordingly, the fluorescence band starts to shift to the red at very low alcohol concentrations. Figure 1b shows the steady-state fluorescence spectra of C153 in hexane/HepOH mixtures at the same alcohol concentrations as in Figure 1a. The normalized shift of the absorption and fluorescence bands are plotted vs the HepOH concentration in Figure 2. From this it can be seen clearly that the fluorescence shift occurs at much lower alcohol concentrations than the absorption shift. At an alcohol concentration of about $x_P = 0.025$ the shift is already 50% of the total fluorescence shift between pure hexane and

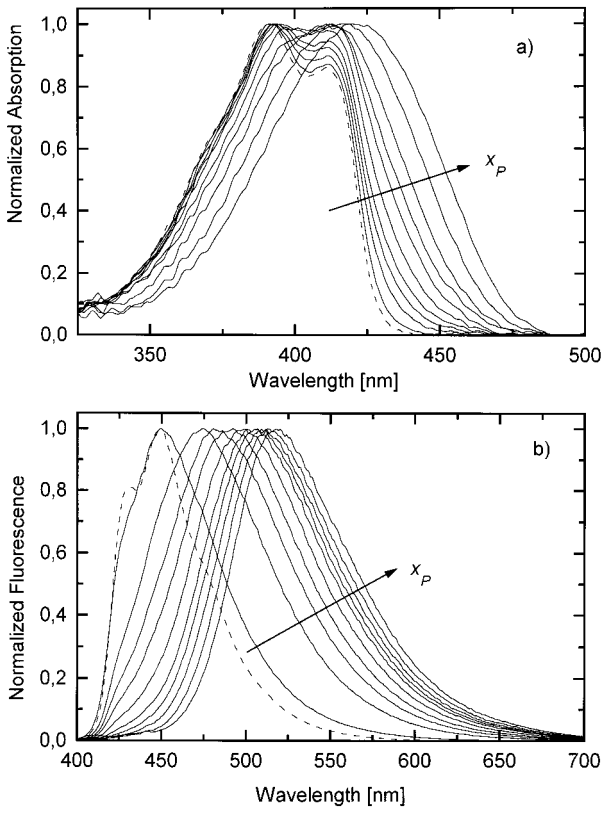

Figure 1. Normalized absorption (a) and fluorescence (b) spectra of C153 in hexane/HepOH mixtures with alcohol mole fractions $x_P = 0$ (dashed line), $x_P = 0.0028$, 0.016, 0.027, 0.048, 0.086, 0.158, 0.238, 0.359, 0.609, 1 (solid lines).

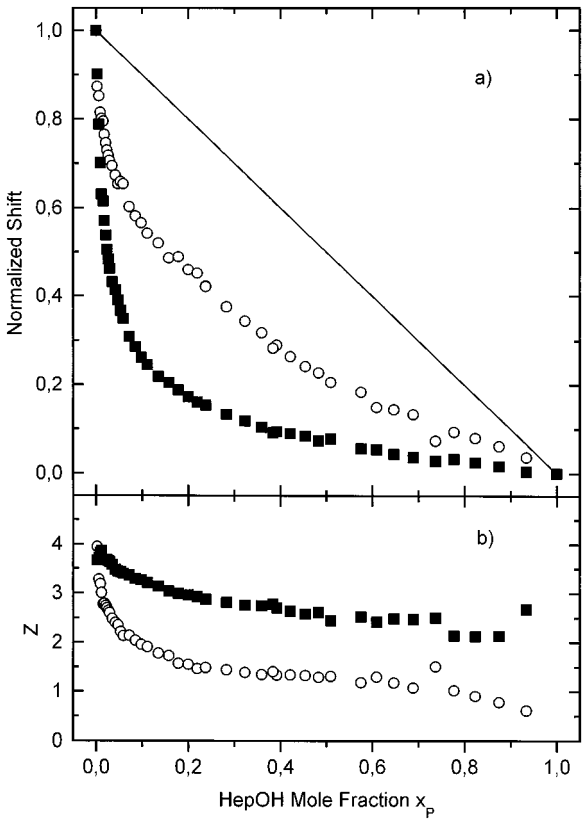

Figure 2. (a) Normalized shift of the center of the steady-state absorption (circles) and fluorescence (squares) spectra of C153 in a hexane/HepOH mixture at different alcohol mole fractions compared to the linear behavior (solid line) expected for homogeneous mixtures according to eq 3. (b) Preferential solvation index Z (eq 13) calculated from the data shown in a.

pure HepOH. The deviation from linear behavior may be measured by[21]

$$\rho = \frac{\int [f_D(x_P) - f(x_P)]\mathrm{d}x_P}{(1/2)\Delta f} \tag{9}$$

where $f_D(x_P)$ is the measured band position at the alcohol mole fraction x_P, $f(x_P)$ is the band position that is expected according to a linear behavior, and Δf is the difference between band positions in pure hexane ($x_P = 0$) and pure alcohol ($x_P = 1$). ρ varies from 0 for ideal mixtures to 1 for complete segregation at infinite alcohol dilution. The values obtained in this way are $\rho_{abs} = 0.32$ and $\rho_{flu} = 0.67$ for ethanol (EtOH) and $\rho_{abs} = 0.46$ and $\rho_{flu} = 0.77$ for HepOH. In all hexane/alcohol mixtures a steep increase of the bandwidth is observed up to an alcohol concentration of about $x_P = 0.05$ (Figure 3). With increasing alcohol concentration x_P the bandwidth decreases gradually to the value that is observed in the pure alcohol.

3.1.2. Steady-State Fluorescence Spectra: Temperature Dependence. The temperature dependence of the steady-state fluorescence spectrum of C153 was studied in a hexane/MeOH mixture at a MeOH mole fraction of $x_P = 0.038$ from 239 to 288 K. The spectra are plotted in Figure 4. A vibronic structure appears on the blue edge of the fluorescence band with decreasing temperature. This structure shows shoulders at approximately the same positions (22 000 cm^{-1} and 23 150 cm^{-1}) where the vibronic bands in pure hexane appear.

3.2. Time-Resolved Fluorescence Measurements. A series of spectra at different times in a hexane/EtOH mixture of $x_P = 0.029$ are shown in Figure 5a together with the static fluorescence spectrum in pure hexane and pure EtOH. The spectra of this mixture are representative of the general behavior of all other mixtures. At very early times the vibrational structure can be observed as in pure hexane, but vanishes later. The shape

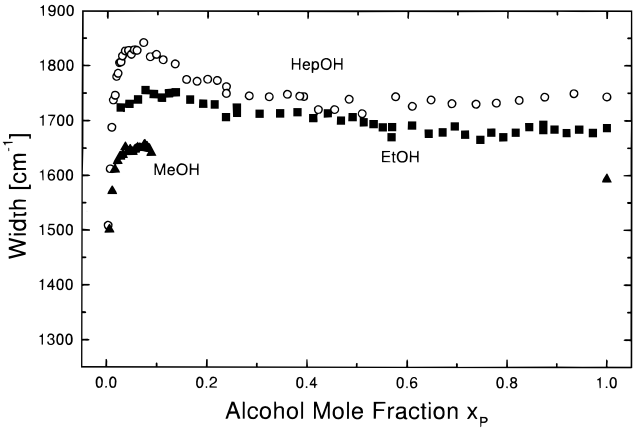

Figure 3. Bandwidth of the steady-state fluorescence spectra of C153 in hexane/MeOH (triangles), hexane/EtOH (squares), hexane/HepOH (circles) mixtures as a function of the alcohol mole fraction x_P.

of the fluorescence band becomes more "alcohol-like". In all our time-resolved fluorescence measurements (TRFM) on alcohol/alkane mixtures the calculated mean values of the spectra (Figure 5b) may be well fitted to a monoexponential decay function

$$\tilde{\nu}_m(t) = \tilde{\nu}_m(0)\mathrm{e}^{-t/\tau_S} + \tilde{\nu}_m(\infty) \tag{10}$$

The width of the fluorescence band at first increases and later decreases (Figure 5c). The time scales on which the changes of these parameters occur depend on temperature, alcohol concentration, and alkane viscosity and are described in more detail in the following sections.

3.2.1. Alcohol/Hexane Mixtures at Different Alcohol Concentrations. The time constant for the time dependent

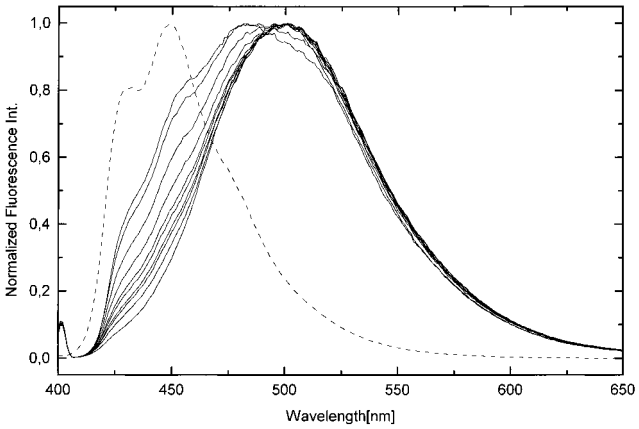

Figure 4. Steady-state fluorescence spectra of C153 in a hexane/MeOH mixture at different temperatures of 288, 274, 268, 265, 260, 256, 248, 239, 227, and 221 K (alcohol mole fraction of $x_P = 0.038$). The dashed line shows the spectrum in pure hexane at room temperature.

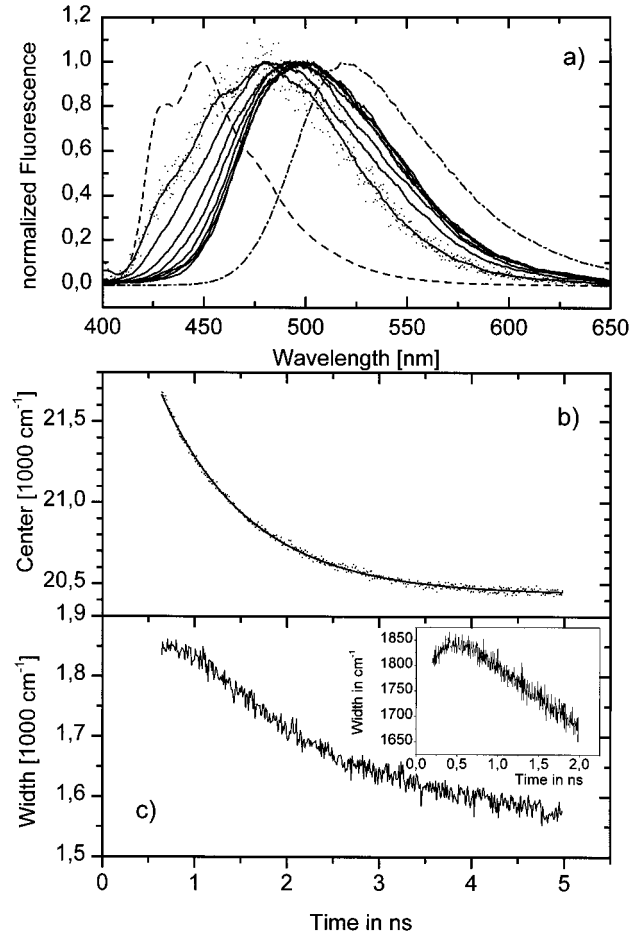

Figure 5. (a) Fluorescence spectra of C153 in a hexane/EtOH mixture at $x_P = 0.029$ at different times ($\Delta t = 0.6$ ns). For the first time step raw data are shown by the dots. The solid lines are the result of smoothing the raw data. Steady-state spectrum in hexane (dashed line) and in pure EtOH (dot−dashed line); (b) center of the band (dots) and monoexponential fit (solid line); (c) width of the band; inset shows data taken with higher time resolution.

Stokes shift of the C153 fluorescence band was measured at different alcohol concentrations. The total observed shift ($\tilde{\nu}(t{=}0) - \tilde{\nu}(t = \infty)$) was 1350, 1340, and 1300 cm^{-1} for MeOH, EtOH, and HepOH. The time constants τ_S decrease steadily with increasing alcohol concentration, spanning a range from 6 ns to 200 ps. They are plotted in Figure 6 as a function of the alcohol concentration. For all three alcohols, approximately the same slope of -0.71 ± 0.05 is observed in the double-logarithmic plot.

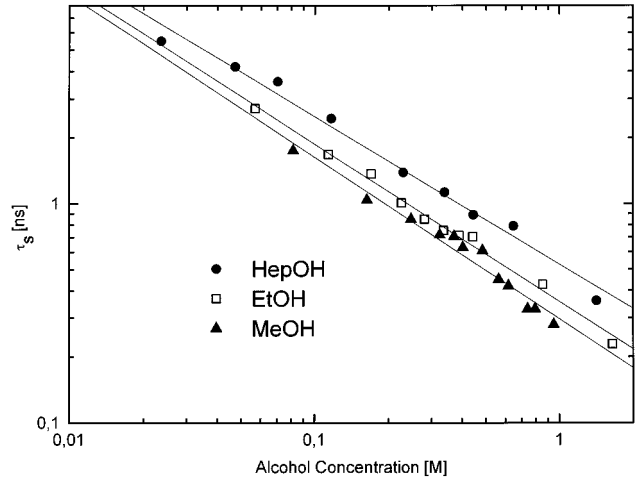

Figure 6. Dependence of the Stokes shift time constants τ_S on the alcohol concentration in hexane/MeOH (triangles), hexane/EtOH (squares) and hexane/HepOH (circles) mixtures. Solid lines: linear fit to the logarithmic data yielding slopes of −0.74, − 0.72, and −0.67 for MeOH, EtOH, and HepOH, respectively.

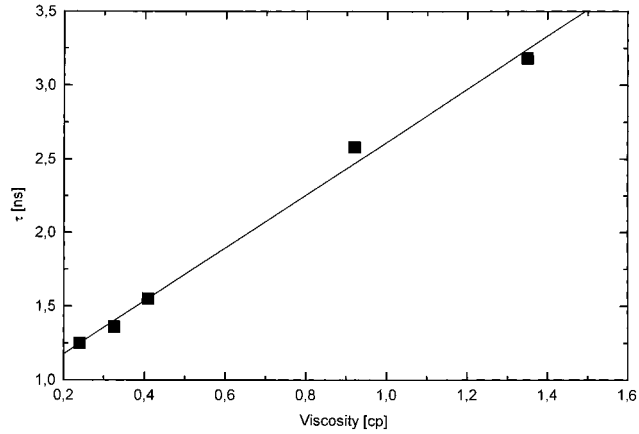

Figure 7. Viscosity dependence of the Stokes shift time constant. The time constants were measured in alkane/EtOH mixtures at an alcohol concentration of 0.17 M ($x_P = 0.022$). The alkanes used were pentane ($\eta = 0.24$ cP), hexane ($\eta = 0.326$ cP), heptane ($\eta = 0.409$ cP), decane ($\eta = 0.92$ cP), and dodecane ($\eta = 1.35$ cP). (Viscosity data are taken from ref 23.)

3.2.2. Effect of Alkane Viscosity. Different alkanes (pentane, hexane, heptane, decane, dodecane) were used to vary the viscosity of the nonpolar part in the mixture at room temperature. The time constants for the Stokes shift were measured for C153 in an alkane/EtOH mixture at an alcohol concentration of 0.17 M ($x_P = 0.022$). The time constants are plotted as a function of the alkane viscosity[23] in Figure 7. An almost perfect linear dependence of τ_S on the viscosity is observed.

The viscosity may also be changed by changing temperature. Therefore the time constants of the Stokes shift were also measured at −30 °C for a hexane/MeOH mixture. Figure 8 shows the spectra at different times. The blue side of the first spectrum is very close to the steady-state spectrum of C153 in pure hexane, showing very similar vibronic structure, but is much broader on the red side. The structure disappears within the next two spectra separated by $\Delta t = 937$ ps. The center of the fluorescence band shifts monoexponentially to lower wavenumbers with a time constant of 6.5 ns. The bandwidth shows a slight increase from 1900 to 1950 cm^{-1} during the first 2 ns and decreases later on to 1600 cm^{-1}, the behavior being qualitatively the same as shown in Figure 5c for EtOH/hexane at room temperature.

3.2.3. Effect of Alcohol Chain Length. To study the influence of the size of the alcohol molecules in the solvation

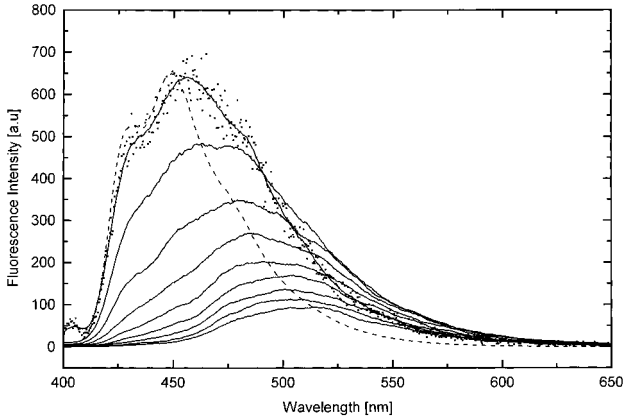

Figure 8. Time-resolved fluorescence spectra of C153 in a hexane/MeOH mixture at $x_P = 0.011$ and $T = 243$ K at different times ($\Delta t = 0.937$ ns). For the first time step raw data are shown by the dots. The solid lines are the result of smoothing the raw data. Steady-state spectrum in pure hexane (dashed line).

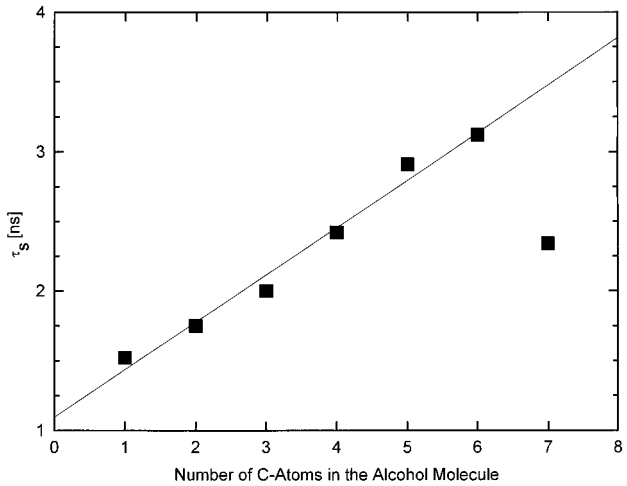

Figure 9. Relaxation times τ_S in dependence on the number of C atoms in the alcohol (concentration 0.11 M ($x_P = 0.014$)) (methanol, ethanol, propanol, butanol, pentanol, hexanol, and heptanol).

dynamics, time-resolved Stokes shift measurements were performed with a series of different alcohols (apart from the already mentioned MeOH, EtOH, and HepOH) at the same volume fraction (of $c_P = 0.01$) in hexane at ambient temperature, namely propanol, butanol, pentanol, and hexanol. To compare the relaxation times at the same concentration of 0.11 M ($x_P = 0.014$, this concentration was used for the butanol measurement), they have been calculated from the concentration dependence as shown in Figure 6 for MeOH, EtOH, and HepOH. Assuming the same dependence (average slope $= -0.71$ in Figure 6) for propanol, pentanol, and hexanol allowed us to extrapolate τ_S at 0.11 M for these alcohols, too. The relaxation times derived from these measurements are depicted in Figure 9. From MeOH to hexanol the measured Stokes shift times vary in an almost perfectly linear manner with the number of carbon atoms in the alcohol.

4. Discussion

Coumarin in the binary alkane/alcohol mixtures studied clearly shows effects of preferential solvation by the alcohol component in the mixture. This can be seen in Figure 2 as the rapid change in band position at very low alcohol concentration, which deviates strongly from the linear behavior expected for the homogeneous mixture. This deviation is much larger for the fluorescence than for the absorption, while there is only little difference between alcohols of different chain length. The general tendency that the number of polar solvent molecules around a solute increases upon excitation of the dye is expected from a simple approximation of the attractive energy between the dipoles of the alcohol and the C153. The dipole−dipole attractive energy (antiparallel dipoles)

$$E_{dd} = \frac{\mu_1 \mu_2}{4\pi\epsilon_0 \epsilon r^3} \tag{11}$$

may be calculated to be 0.026 eV for the ground state (using $r = 5.2$ Å, $\epsilon = \epsilon_{hexane} = 1.88$, μ_1(EtOH) = 1.7 D, μ_2(C153) = 6.6 D, and $E_{dd} = 0.059$ eV for the excited state (μ_2(C153*) = 15 D). For the ground state E_{dd} is comparable to the thermal energy E_{therm} of 0.026 eV. Therefore a solute−solvent aggregate will be easily destroyed, while it will be much more stable in the excited state, where E_{dd} is approximately 2 times E_{therm}.

In a more accurate picture, entropy, which favors separation, needs to be taken into account, as was done by Suppan.[21] Before discussing this in more detail we would like to comment on the behavior of the Onsager function $f(\epsilon)$ of the pure solvent mixture (without solute). This has to be taken into account, as even in this case there is not necessarily a linear correlation with x_P. Measurements of the dielectric constants of solvent mixtures are not available for the system under investigation. Data on similar systems are scarce, especially in the low concentration range. Measurements for propanol in cyclohexane and butanol in cyclohexane[24] at a few mixing ratios with $x_P > 0.3$ indicate a deviation from linear behavior ($\rho \approx 0.2$). On the other hand, for EtOH in cyclohexane at $x_P < 0.02$ the Onsager function derived from dielectric measurements[25] follows almost exactly the ideal linear behavior as a function of x_P. As shown by the data of F. Köhler[26] for heptanol in pentane, extending over the whole concentration range ($x_P = 0, ..., 0.1$), both behaviors may be present in one solvent mixture, the deviation from linearity being effective only for $x_P > 0.2$. This indicates, of course, that the solvent structure as a function of x_P is rather complicated. Due to this uncertainty, we do not consider deviations from linear behavior of $f(\epsilon)$ for the solvent mixture.

The increase of the ratio of the mole fraction of alcohol (y_P) and of alkane (y_N) in the solvent shell as compared to that of the ratio in the bulk (x_P/x_N) we will denote as β.

$$\beta = [(y_P)/(y_N)]/[(x_P/x_N)] \tag{12}$$

According to, ref 21, a preferential solvation index Z can be defined as $\beta = e^Z$. Z may be calculated according to

$$Z = \frac{1}{4\pi\epsilon_0} \frac{C\mu^2 M \Delta f(\epsilon)_{N,P}}{2\pi RT\delta r^6} \tag{13}$$

where C is a numerical constant on the order of unity, μ is the solute dipole moment, M is the mean molar weight of polar and nonpolar solvent, Δf is the difference of the Onsager functions of pure polar and pure nonpolar solvent ($\Delta f = f(\epsilon_P) - f(\epsilon_N)$), R is the gas constant, T is the temperature, δ is the mean density of the two solvent components, and r is the mean distance between the solute and the solvent molecules of the solvation shell. Using for EtOH/hexane mixtures $M = 66.13$ g mol^{-1}, $\delta = 0.725$ g cm^{-3}, $\mu_{C153} = 6.6$ D, and $r = 5.2$ Å leads to $Z = 2.38$, i.e., to $\beta = 10.8$. (The radii of the solvent and solute molecule were defined using a sphere with a volume equal to that of the (smallest) rectangular boundary box of the molecule.)

We calculated β from the concentration dependence of the center of fluorescence and absorption as shown in Figure 2. As

the concentration of C153 is much lower than that of the alcohol, even at the lowest alcohol concentration, x_P is equal to the mole fraction of alcohol in the sample. y_P is derived as that mole fraction for which linear behavior would lead to the same shift as observed. The values obtained for $Z = ln(\beta)$ are shown in Figure 2b. In contradiction to simple theory they are not constant but show a pronounced decrease from approximately 4 to 2.5 and from 4 to 0.5 for fluorescence and absorption, respectively. The size of Z is comparable to the theoretical value, but we want to point out that it depends on the sixth power of r, therefore being very sensitive to the choice of r. The coincidence is therefore due to a good choice of r. Furthermore, according to eq 13, Z should be higher by a factor of 5 for the excited state ($\mu = 15$ D) as compared to the ground state ($\mu = 6.6$ D). This is in contradiction to the factor 2 we found between Z derived from fluorescence and absorption measurements. We therefore conclude that the theoretical model discussed is much too simple to quantitatively describe preferential solvation in the solute−solvent systems under investigation. Obviously a more detailed microscopic theory, taking specific solute−solvent interactions into account would be necessary.

Nevertheless the steady-state spectra clearly show that the concentration of alcohol in the solvent shell is higher in the excited state as compared to the ground state. We suppose that in order to fill up the solvation shell alcohol molecules must diffuse to the excited C153 molecules, where they will be trapped, thus leading to the increased preferential solvation observed in fluorescence.

This also explains the steady-state spectra at low temperatures. Bands like in pure hexane are clearly observed at the blue side of the fluorescence band. This means that at these temperatures the time needed for the change of the solvation shell is comparable to the fluorescence lifetime. If there was no diffusion but stabilization of an at room-temperature already existing solvent shell, no such effect but rather a red-shift would be expected at low temperatures.

The time scale at which this diffusion process occurs as well as the concentration dependence may be understood from statistical mechanics. The mean squared displacement of a molecule from its origin is given by[30]

$$\bar{r}^2 = 6Dt \tag{14}$$

Here D is the diffusion coefficient of the considered species and t is the time. The mean distance $\bar{r}$ between two MeOH molecules is given by the number of molecules per volume d. This corresponds also to the order of magnitude of the C153−MeOH distance if the C153 concentrations is much lower than the MeOH concentration.

$$\bar{r} = d^{-1/3} \tag{15}$$

Equations 14 and 15 lead to

$$\tau_{diff} = \frac{1}{6Dd^{2/3}} \propto \tau_S \tag{16}$$

where τ_{diff} represents the time needed for MeOH to arrive at the C153 molecule. According to this, a diffusion-controlled solvation process should result in a time constant that follows the concentration with $d^{-0.67}$. This is exactly what is experimentally observed for HepOH (Figure 6). The shorter alcohols MeOH and EtOH show a steeper slope of −0.74 and −0.72. This could be related to an increased clustering of shorter alcohols. The found concentration dependence of the solvation process differs from the linear dependence of the reaction rate known from simple bimolecular reactions. This is because the bimolecular reaction rate represents the number of events per unit time in equilibrium and not of a starting "reaction" as observed in the experiment. The experiment is therefore determined by the time needed to travel to the C153 as described above and not by an average equilibrium time between two events. From eq 16 τ_{diff} may be estimated to be approximately 200 ps for $d = 1.51 \times 10^{26}$ m^{-3} ($x_P = 0.01$ MeOH) and $D = 3 \times 10^{-9}$ m^2 s^{-1} (typical values are 3.7×10^{-9}, 4.21×10^{-9}, and 2.73×10^{-9} m^2 s^{-1} for CCl_4, toluene, and dodecane in hexane). In a simple model we may describe the solvation process by

$$\frac{dN_B(t)}{dt} = k\frac{N_B^{inf} - N_B(t)}{N_B^{inf}} \tag{17}$$

where $N_B(t)$ is the number of alcohol molecules around one dye molecule. N_B^{inf} is this number at infinite time. This ansatz takes into account a reduced probability for an alcohol molecule to stick to an already existing solute solvent complex with a growing number of alcohol molecules in this complex. The solution of eq 17 leads to

$$N_B(t) = N_B^{inf}(1 - e^{-\tilde{k}t}) \tag{18}$$

with $\tilde{k} = k/N_B^{inf}$. Taking for k the above-described $(\tau_{diff})^{-1}$ and $N_B^{inf} = 5$ (estimated from approximately 10 molecules in the first solvation shell which at $x_P = 0.01$ is approximately half filled, see Figure 2) leads to $\tilde{k}^{-1} = 1$ ns. This is the correct order of magnitude compared to the measured value of 1.75 ns for MeOH. Rotational correlation times which account for the diffusive part of solvent relaxation in pure alcohol solution are 1−2 orders of magnitude smaller (5 and 16 ps average relaxation time are given for MeOH and EtOH, respectively[9]). There is therefore no doubt that the observed relaxation times are due to translational and not rotational diffusion. Nevertheless the latter should be of significance for the alcohol molecules which are already in the ground-state solvation shell. Due to our presently limited time resolution, short times cannot be resolved in our experiments. The dependence of τ_S on the length of alcohol molecules (Figure 9) also supports translational diffusion. The measured values vary almost linearly with the size of the molecule. According to the Stokes−Einstein relation, the diffusion coefficient for translational motion varies with r^{-1}, and therefore the collision times are expected to be linear in r^{-1} too. On the other hand, for rotational correlation times, a r^{-3} dependence is expected. Indeed, the average relaxation times in pure alcohols do show approximately a cubic dependence on the number of carbon atoms in the chain.[9] A more detailed model would take a multistep reaction scheme into account:

$$A \underset{k_{-1}}{\overset{k_1}{\rightleftharpoons}} AB_1 \underset{k_{-2}}{\overset{k_2}{\rightleftharpoons}} AB_2 \underset{k_{-3}}{\overset{k_3}{\rightleftharpoons}} \ldots \underset{k_{-10}}{\overset{k_{10}}{\rightleftharpoons}} AB_{10}$$

This describes the formation of solute−solvent aggregates including backward reaction rates k_{-i}. (The alcohol molecules in the bulk are not included in the reaction scheme.) Thus we deal with a mixture of C153 molecules surrounded by a different number of alcohol molecules. The spectrum at a certain time is a superposition of the spectra of different solute−solvent complexes weighted by their respective concentration. In the beginning only gound-state-like surroundings contribute to the spectrum, while later different surroundings leading to different spectral positions are simultaneously present. Finally all molecules will end up with the same saturated solvation shell. This more detailed model of aggregates with different solvent shells describes well the behavior of the time-resolved spectra

(Figure 5a). At the beginning the hexane-like structure is resolved, but vanishes due to the rearrangement of the solvent shell during time evolution. The time dependent width of the spectrum can be understood from this model as well: At the begining the narrow hexane-like spectrum dominates. At later times different aggregates contribute to a broader spectrum, which finally narrows to that of the equilibrium state. Due to the limited time resolution, most of the risetime of the width cannot be observed. In principle it would be expected to start approximately at the value of pure hexane of 1300 cm^{-1}. As the diffusivity of the alcohol in alkane is lowered by increasing either the size of the alcohol or the viscosity of the alkane, the increase of the width can best be seen for longer alcohols (EtOH better than MeOH), longer alkane chains (EtOH in dodecane better than EtOH in pentane), or at low temperatures (Figure 8).

5. Conclusions

Concluding from the results discussed, it can be said that the measured solvation dynamics in alcohol/alkane mixtures is determined by a diffusion process which leads to a preferential solvation in the excited state of Coumarin 153. As the whole process is not simply described by diffusion of single alcohol molecules in a nonpolar alkane, further studies are needed to show the solvation dynamics in more detail. For instance, it is necessary to consider aggregation of alcohol molecules due to hydrogen bonding at low concentrations.[27−29] As the dipole moment and the diffusivity of such dimers or tetramers decreases, mainly the monomers are expected to take part in the solvation process. Since an increasing amount of dimers and tetramers lowers the monomer concentration, one could observe effects of the aggregation (i.e. a structure) in the concentration dependence of the Stokes shift time constants. Additionally a detailed line shape analysis of the absorption and fluorescence will probably give more information about the distribution of differently solvated C153 molecules. Molecular dynamics simulations are in progress to understand better the preferential solvation.

Acknowledgment. This work was supported by the Deutsche Forschungsgemeinschaft within the Schwerpunkt “Schnelle molekulare Prozesse in Flüssigkeiten” and by a scholarship of the Freistaat Sachsen for F. C. Discussions with R. Brown, Université de Bordeaux I, are gratefully acknowledged.

References and Notes

(1) Reichardt, C. *Solvents and Solvent Effects in Organic Chemistry*; VCH: Weinheim, 1990.
(2) Liptay, W. *Z. Naturforsch.* **1965**, *20a*, 1441.
(3) Suppan, P. *J. Photochemi. Photobiol., A: Chem.* **1990**, *50*, 293.
(4) Mataga, N.; Kaifu, Y.; Koizumi, M. *Bull. Chem. Soc. Jpn.* **1956**, *29* (4), 465.
(5) Bilot, L.; Kawski, A. *Z. Naturforsch.* **1962**, *17a*, 621−627.
(6) Banerjee, D.; Laha, A. K.; Bagchi, S. *J. Photochem. Photobiol. A: Chem.* **1995**, *85*, 153−159.
(7) Nagarajan, V.; Brearley, A. M.; Kang, T.-J.; Barbara, P. F. *J. Chem. Phys.* **1987** *86* (6), 3183.
(8) Maroncelli, M.; MacInnis, J.; Fleming, G. R. *Science* **1989**, *243*, 1674.
(9) Horng, M. L.; Gardecki, J. A.; Papazyan, A.; Maroncelli, M. *J. Phys. Chem.* **1995**, *99*, 17311−17337.
(10) Gustavsson, T.; Baldacchino, G.; Mialocq, J.−C.; Pommeret, S. *Chem. Phys. Lett.* **1995**, *236*, 587−594.
(11) Maroncelli, M.; Fleming, G. R. *J. Chem. Phys.* **1987**, *86* (11), 6221.
(12) Jarzeba, W.; Walker, G. C.; Johnson, A. E.; Barbara, P. F. *J. Chem. Phys.* **1991**, *152*, 57.
(13) Simon, J. D. *Acc. Chem. Res.* **1988**, *21*, 128.
(14) Rosenthal, S. J.; Xie, X.; Du, M.; Fleming, G. R. *J. Chem. Phys.* **1991**, *95* (6), 4715.
(15) Kahlow, M. A.; Kang, T. J.; Barbara, F. *J. Chem. Phys.* **1988**, *88*, 2372.
(16) Chapman, C. F.; Fee, R. S.; Maroncelli, M. *J. Phys. Chem.* **1995**, *99*, 4811−4819.
(17) Fourkas, J. T.; Berg, M. *J. Chem. Phys.* **1993**, *98* (10), 7773.
(18) Fourkas, J. T.; Benigno, A.; Berg, M. *J. Chem. Phys.* **1993**, *99*, 8552.
(19) Reynolds, L.; Gardecki, J. A.; Franland, S. J. V; Horng, M. L.; Maroncelli, M. *J. Phys. Chem.* **1996**, *100*, 10337.
(20) Petrov, N. Kh.; Wiessner, A.; Fiebig, T.; Steark, H. *Chem. Phys. Lett.* **1995**, *241*, 127−132.
(21) Suppan, P. *J. Chem. Soc., Faraday Trans. 1* **1987**, *83*, 495.
(22) Bingemann, D.; Ernsting, N. P. *J. Chem. Phys.* **1995**, *102* (7), 2691.
(23) Lide, D. R. *Handbook of Chemistry and Physics*; CRC Press: Boston, 1990.
(24) Magallanes, C. *J. Mol. Liq.* **1991**, *50*, 53.
(25) Ibbitson, D. A.; Moore, L. F. *J. Chem. Soc. (B)* **1967**, 76.
(26) Köhler, F. Diploma Thesis, Universität Göttingen, 1995.
(27) Campbell, C.; Brink, G.; Glasser, L. *J. Phys. Chem.* **1975**, *79* (6), 660.
(28) Brink, G.; Glasser, L. *J. Phys. Chem.* **1978**, *82*, 1000.
(29) Fletcher, A. N. *J. Phys. Chem.* **1972**, *76*, 2562.
(30) Chaikin, P. M.; Lubensky, T. C. *Priciples of Condensed Matter Physics*; Cambridge University Press: Cambridge, 1995.